small NANO MICRO

Carbon nanotubes

DOI: 10.1002/smll.200800082

Phase Behavior and Shear Alignment in SWNT-Surfactant Dispersions

*Einat Nativ-Roth, Rachel Yerushalmi-Rozen, and Oren Regev**

***T**he effect of single-walled carbon nanotubes (SWNT) on the phase behavior of the cationic surfactant cetyltrimethylammonium bromide (CTAB) in aqueous solutions is investigated at room temperature. Small-angle X-ray scattering (SAXS) and cryogenic transmission electron microscopy (cryo-TEM) are used for characterization of bulk dispersions and nanometrically thin films. Additional carbonaceous additives (fullerenes, multi-walled carbon nanotubes, and carbon black) serve as reference systems. It is found that dispersions of carbonaceous additive (excluding fullerenes) at intermediate surfactant concentrations (below the liquid-crystalline region of the native surfactant) induce demixing and macroscopic phase separation in otherwise homogeneous solutions of CTAB. Two coexisting liquid phases of similar CTAB concentrations are observed, with the carbonaceous species residing within the lower phase. At high CTAB concentrations (liquid-crystal region) the SWNTs are found to incorporate into the ordered lyotropic liquid-crystalline phase while preserving the native d-spacing. Investigation of nanometrically thin films at intermediate surfactant concentrations under external shear reveals shear-induced structure (SIS) in the presence of minute amounts of SWNTs. The effect is found to be exclusive to SWNT and does not occur in dispersions of other carbonaceous additives.*

Keywords:
- carbon nanotubes
- cryo-TEM
- CTAB
- shear alignment
- SAXS

1. Introduction

Single-walled carbon nanotubes (SWNT) are nanostructures characterized by a typical diameter that lies between the upper limit of large molecules and the lower limit of small colloidal particles and a persistence length of the order of micrometers.[1,2] Utilization of SWNT relies on the ability to disperse them in liquid media and control their behavior in different environments. Dispersion protocols of SWNTs in aqueous solutions contemplate the utilization of ionic surfactants at low concentrations[3–5] for formation of stable dispersions of individual tubes. Yet surfactant molecules are known to exhibit rich phase diagrams at concentrations above the critical micellar concentration (CMC). Upon increasing the concentration, elongated micelles may become stable and further aggregate and orient into lyotropic liquid-crystal (LC) phases. It has been suggested that inclusion of SWNTs within lyotropic LC phases would open a wealth of possibilities, as LC phases are important in a variety of applications, ranging from cosmetics, paints, to molecular sensors.[6–9]

[*] Prof. O. Regev, Prof. R. Yerushalmi-Rozen
Department of Chemical Engineering and
The Ilse Katz Institute for Nanoscale Science and Technology
Ben-Gurion University of the Negev
Beer Sheva 84105 (Israel)
Fax: +972-8-6472916
E-mail: oregev@bgu.ac.il
E. Nativ-Roth
Department of Chemical Engineering
Ben-Gurion University of the Negev
Beer Sheva 84105 (Israel)

Supporting Information is available on the WWW under http://www.small-journal.com or from the author.

The interaction between LC phases and nanostructures is nontrivial. Previous experiments on lamellar LCs indicate that the presence of additives affects the elastic constants of the LC phase. It was shown that spherical particles are stable within the lamellar LCs only if the bilayers are soft and fluctuating.[10,11] In hexagonal LCs, the additives were found to be depleted from the inner walls of the cylinders.[12] Other studies reported that additives change the phase boundaries of the LCs[13] or their spacing.[14]

Here, we investigate the effect of SWNTs on the phase behavior of an anisotropic molecule (cetyltrimethylammonium bromide (CTAB)) in aqueous solutions at room temperature. We study both bulk solutions and thin films and focus on shear-induced structures (SIS) formed in nanometrically thin films of SWNT–CTAB–water dispersions at room temperature.

2. Results

The room temperature phase behavior of the combined SWNT–CTAB–water system, in bulk and ultrathin film configurations was investigated using small-angle X-ray scattering (SAXS) and cryogenic transmission electron microscopy (cryo-TEM). Studies of fullerenes, multi-walled carbon nanotubes (MWNTs), and carbon black (CB) dispersions were carried out for comparison.

2.1. Bulk Solutions

2.1.1. Characterization of the Ternary SWNT–CTAB–Water System

The effect of SWNT additives (0.1 wt %) on aqueous dispersions of CTAB was examined at CTAB concentration range of 0.5–30 wt %. Three different regimes could be distinguished: A lower concentration regime, $C_{CTAB} < 5$ wt %, an intermediate regime, 5 wt % $< C_{CTAB} <$ 22 wt % and concentrated regime, $C_{CTAB} > 22$ wt %. At the lower concentration regime a single phase of macroscopically homogeneous black, inklike dispersion was observed. At the intermediate region two liquid phases coexisted: A transparent upper phase that contains almost no SWNTs, and a lower phase composed of well-dispersed SWNTs (see inset of Figure 1). A re-entrant single phase of black inklike dispersion was observed in the concentrated regime.

The intermediate, two-phase region was examined in detail. The volume of the two phases was found to depend on the concentration of both CTAB and SWNT, where the volume of the lower phase was higher for either higher CTAB concentration (at fixed SWNT concentration) or higher SWNT concentration (at fixed CTAB concentration). The overall CTAB concentration was found to be similar in the two phases.

The dispersions were found to be stable over long incubation periods (at room temperature), retaining their inklike texture. Cryo-TEM micrographs indicate that the SWNT are dispersed as individual tubes or small bundles in the CTAB solutions (see below). The dispersed SWNT did not coagulate with time or centrifugation.

A similar behavior was observed in dispersions of MWNT and CB at similar concentrations, whereas dispersions of fullerenes did not exhibit demixing but rather retained a single-phase behavior throughout the whole concentration regions.

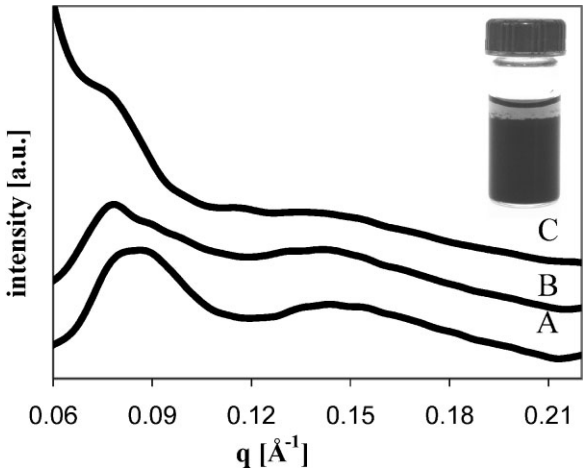

Figure 1. SAXS patterns of aqueous solutions of 15 wt % CTAB. A) The native solution. B) The upper phase taken for a C_{SWNT} (0.1 wt %)–C_{CTAB} (15 wt %)–water dispersion. C) The lower phase of the same dispersion as in (B). Inset: a picture of the SWNT–CTAB–water two-phase system.

The ternary SWNT–CTAB–water system was characterized using SAXS. In Figure 1, we present scattering curves of the two phases comprising the C_{SWNT} (0.1 wt %)– C_{CTAB} (15 wt %)–water system. A scattering curve of an aqueous solution of CTAB (15 wt %) is presented for comparison (Figure 1A). While the scattering curve of the upper phase of the ternary system is similar to that of the native CTAB solution of a similar concentration, that of the lower phase (Figure 1C) is distinguished by high scattering at low q values, typical for rodlike dispersions.[15] The absence of the latter in the scattering curve of the upper phase is another indication that SWNT are depleted from the upper phase.

In the concentrated surfactant regime (CTAB concentration of 22–30 wt %) SWNT (of concentrations ranging from 0.05 to 0.4 wt %) form black, homogeneous single-phase dispersions. Scattering curves (Figure 2) indicate that the presence of SWNT neither modifies the symmetry of the surfactant phase nor does it affect its d-spacing. The domain size of the hexagonal phase was calculated using the Sherrer formula[16] and is found to be ~100 nm for all samples, irrespective of the presence of SWNT.

We note that CB additives could not be dispersed in the LC surfactant phases at similar concentrations, and CB powder precipitated at the bottom of the vials.

2.1.2. Characterization of the Binary CTAB–Water System

The bulk-phase diagram of CTAB in water has been thoroughly investigated before.[18,19] At room temperature the CMC occurs at C_{CTAB} of 0.03 wt%,[20] where spherical micelles form. A transition to rodlike micelles takes place at C_{CTAB} of 12 wt%[20] followed by a transition to a nematic region at CTAB concentration of 22 wt% and a hexagonal phase at concentrations above 25 wt% (Scheme 1). Visual inspection through crossed polarizers indicates that our

small

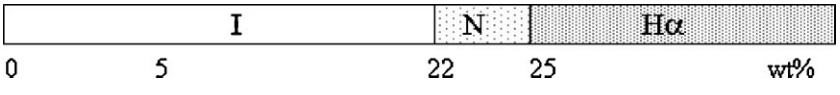

Scheme 1. Phases observed in aqueous solutions of CTAB at 25 °C (wt %). I, isotropic; N, nematic; Hα, hexagonal.

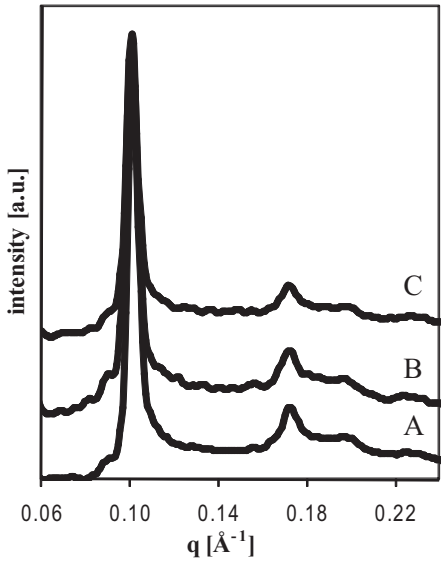

Figure 2. SAXS patterns of the hexagonal phase at C_{CTAB} (29 wt %): A) the native CTAB solution without SWNT (in agreement with pervious studies), [17] with B) C_{SWNT} (0.1 wt %), C) C_{SWNT} (0.2 wt %).

CTAB–water system follows the expected behavior: solutions up to CTAB concentrations of 22 wt% are optically isotropic,[21] a nematic phase appears at 22 wt% and is followed by a hexagonal phase at 25 wt%.

2.2. Nanometrically Thin Films

Ultra thin films were characterized via cryo-TEM microscopy. Specimens for TEM imaging are prepared using a vitrification robot system (Vitrobot, see below). The preparation procedure involves placing a microdroplet on electron microscopy (EM) grid, blotting the excess liquid[22] and ultrafast thermal quenching (at typical cooling rates in the range of 10^5 K s^{-1}[23]) to a final temperature of −180 °C. It is well known that blotting exerts strong shear forces (10^3–10^6 s^{-1})[22,23] on the film. As suggested by earlier studies SIS and on-the-grid structural transitions are often observed in cryo-TEM experiments.[22,24] Among the reported shear-induced structural transitions are from micelles to bilayers, spherical micelles-to-elongated, elongated micelles-to-vesicles,[22] as well as the reversed direction.[24]

A vitrification robot system (Vitrobot[25]) is a guillotine-like device. The EM grid is held by tweezers attached to a rod. A droplet of liquid is placed on the grid and automatically blotted by two disks covered by filter papers in a ''clamping hands'' configuration. The apparatus is enclosed in a controlled temperature and humidity chamber. After the blotting action the rod-loaded sample is plunged into a coolant, transferred to the microscope and imaged under cryogenic conditions. The Vitrobot enhances the control of the blotting force exerted on the samples, the number of blotting actions and their duration, and enables one to explore in a reproducible manner the nonequilibrium SIS in the SWNT–CTAB–water system.

2.2.1. Characterization of the Ternary SWNT–CTAB–Water System

Ultra thin films (5–100 nm thick) were prepared in the vitrobot[26] and examined by cryo-TEM.

In Figure 3A, we present cryo-TEM micrographs of the lower phase of SWNT–CTAB–water dispersion in the intermediate regime (see Figure 1 inset). For comparison, thin films prepared from the upper phase (Figure 3B) and from the native CTAB solution (Figure 3C) are presented. We observe that the dominant features in the SWNT-containing phase are long cylindrical CTAB micelles (different from bilayer structure[27]) with a contour length of few hundreds of nanometers to about a micron. The elongated micelles are aligned parallel to the longer SWNT (having a higher electron density (vide infra), and indicated by arrows in Figure 3A). Large areas of mutually parallel micelles form large arrays of an ordered phase over areas of typically a few micrometers.

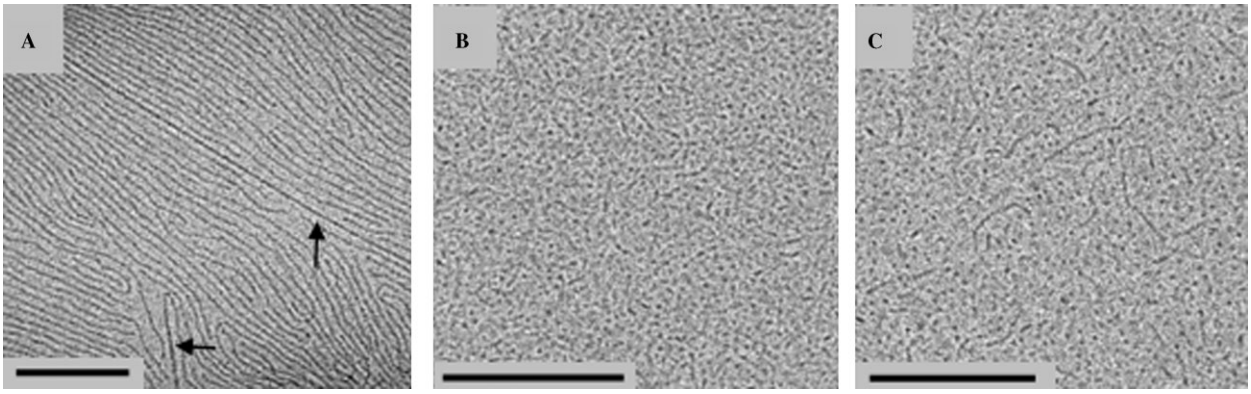

Figure 3. Cryo-TEM micrographs of an aqueous dispersion of C_{SWNT} (0.1 wt %)–C_{CTAB} (9 wt %). A) The lower phase, B) the upper phase, C) a native aqueous solution of C_{CTAB} = 9 wt %. Scale bar 200 nm. Black arrows point at SWNT.

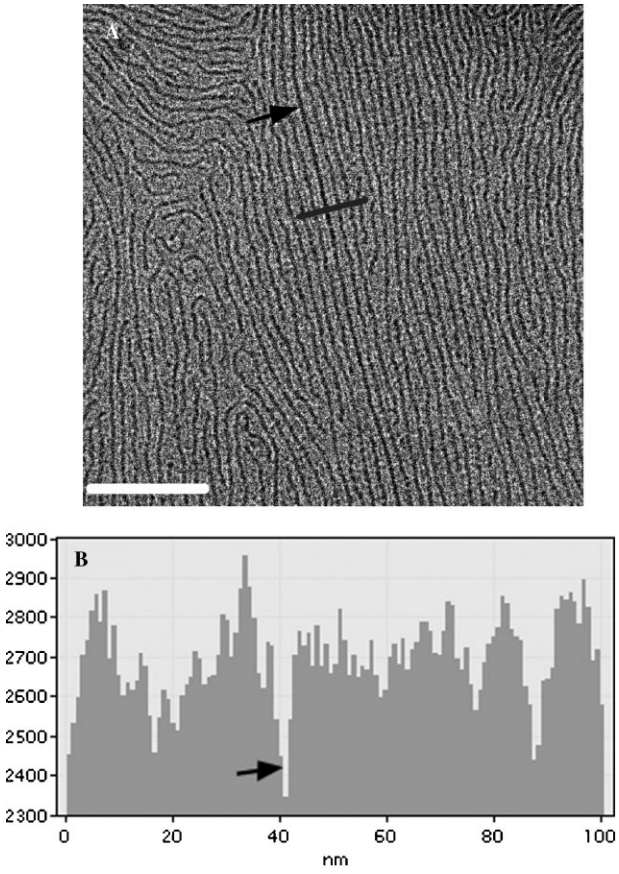

Figure 4. A) Cryo-TEM micrograph of the lower phase of a C_{SWNT} (0.1 wt %)–C_{CTAB} (12 wt %)–water dispersion. B) Electron densitometry map along the black line in (A) showing the contrast of a SWNT (indicated by an arrow) and CTAB micelles. The ordinate values are electron counts. Scale bar 200 nm.

When two nonaligned SWNTs are present in close vicinity (black arrows in Figure 3A), we observe a shift in the micellar orientation according to the distance from the tube: while micelles in the vicinity of one SWNT follow its contour length, micelles near the other SWNT are aligned parallel to it. Note that the micelles may bend and their spacing may change so as to follow the SWNT contour (another example can be seen in Figure 5B). Very differently, micrographs of the native CTAB solution and the upper phase (Figure 3B and C) show mostly spherical micelles, with some short cylindrical micelles.

A similar behavior is observed for SWNT–CTAB–water dispersions in the $9 \leq C_{CTAB} < 15$ wt % range.

In Figure 4, we present a densitometry analysis of a characteristic TEM micrograph where both CTAB-coated SWNT and native CTAB micelles are present. In Figure 4A, the micelles and the SWNT appear as dark lines, separated by light regimes of vitrified water. As the mass-thickness contrast in TEM stems from differences in electron density, the water appears bright and the micelles and SWNTs are darker. In general, carbon nanotubes are electron-dense objects (10^{17} m^{-3})[28] due to their structure, resulting in a high contrast relative to the CTAB micelles (Figure 4B).

2.2.2. Probing the Origins of Micelle Ordering and Alignment

To investigate the driving force for the appearance of an ordered phase of mutually parallel micelles (Figure 3A) we performed three series of experiments. In the first series, we studied the effect of additives of similar compositions, surface chemistry and specific surface area, but of different dimensions (MWNT) and geometry (CB) on the phase behavior of CTAB. In the second series, we examined the phase behavior at different CTAB concentrations. These native systems serve as a control: by studying their structure we could draw a base-line for the behavior of additive-free systems. In the third series, we performed a set of on-the-grid post-shear relaxation experiments, in which the blotted samples were allowed to relax before quenching.[24] In the following we present the results.

Figure 5 presents cryo-TEM micrographs prepared from dispersions of CTAB (10 wt %) and different carbonaceous additives: CTAB solution with no additives (Figure 5A), with SWNT (Figure 5B), MWNT (Figure 5C), and CB (Figure 5D). We clearly observe that under similar sample preparation conditions SWNT induce orientational ordering of elongated CTAB micelles whereas MWNT nor CB do not.

Figure 6 summarizes the phase behavior of liquid films prepared from the native aqueous solutions of CTAB at concentrations of 9, 12, and 15 wt %. The micrographs reveal an evolution from dominance of spherical micelles with an occasional appearance of cylindrical micelles at $C_{CTAB} = 9$ wt % (Figure 6A) to dominance of nonoriented cylindrical micelles at $C_{CTAB} = 12$ wt % (Figure 6B), in agreement with previous studies.[20] Note the high flexibility of the micelles at 12 wt %. Specimens prepared from solutions of $C_{CTAB} =$ 15 wt % (Figure 6C) are dominated by elongated micelles that are aligned with respect to each other, and separated by narrow regions of vitrified solution. Higher concentrations of CTAB solutions could not be imaged by cryo-TEM.[29]

The results obtained from the first two sets of experiments described above suggest that orientational ordering in sheared thin films (Figure 6C) significantly precedes the fully ordered phase in the nonsheared bulk and takes place already at $C_{CTAB} =$15 wt % (cryo-TEM) as compared to $C_{CTAB} =$ 22 wt % observed in the bulk (SAXS).[21] The presence of SWNT induces preferential in-plane alignment, and elongated, well-aligned micelles appear already at $C_{CTAB} \sim 9$ wt %. The micelles exhibit a long contour length and form large areas of micelles aligned along SWNT. The distribution of intermicellar spacing is much broader when alignment is induced by SWNT, as compared to concentration induced alignment in the native films ($C_{CTAB} > 15$ wt %).

Semiquantitative structural analysis of the species observed in the cryo-TEM micrographs of the different systems is presented in Table S1 in the Supporting Information.

We observe that the diameter of individual SWNT coated by adsorbed CTAB molecules is similar to that of a native CTAB micelle ~5 nm (Figure 4). We believe that dimensional matching plays a crucial role in SWNT-nucleated micelle alignment and orientational ordering, and relate to it in detail in the discussion.

small NANO MICRO

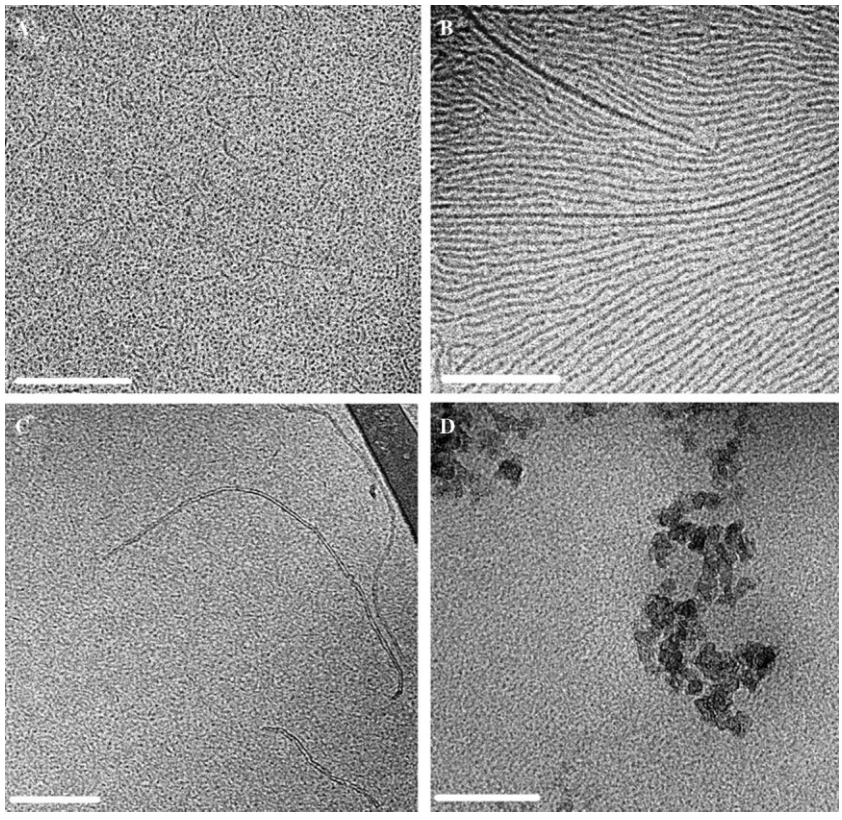

Figure 5. Cryo-TEM micrographs of C_{CTAB} (10 wt %) solution. A) The native solution, B) dispersion of C_{SWNT} (0.1 wt %), C) dispersion of C_{MWNT} (0.1 wt %), D) dispersion of C_{CB} (0.1 wt %). Scale bar 200 nm.

To investigate the effect of shear history on the CTAB–water binary system and SWNT–CTAB–water ternary system we performed the third set of experiments. Ultra thin films were prepared by blotting a droplet of the solution (or dispersion), previously deposited on the TEM grid, as described in the experimental part. Following the blotting stage, the samples were allowed to relax for different periods of times, ranging from 0 to 90 s. During the relaxation time temperature and maximal relative humidity were well controlled.

CTAB–Water Binary System: A series of specimens prepared from the same solution of C_{CTAB} (15 wt %) following different relaxation periods (0, 40, and 90 s) were imaged by cryo-TEM and the effect of relaxation time on micelles alignment was analyzed. In Figure 7, we present two typical micrographs following a relaxation period of 0 s (Figure 7A) and 90 s (Figure 7B). We found that the area of the ordered regions increases significantly after a relaxation period of 90 s (as compared to the nonrelaxed samples). In addition, we found that the typical spacing between micelles (d-spacing) decreases by about 1 nm (from 12.8 to 11.9 nm). Statistical analysis of the data suggests that the standard deviation of the inter-micellar spacing decreases as the on-the-grid post blotting relaxation period increases (Figure 7C).[30]

SWNT–CTAB–Water Ternary System: Series of specimens prepared from dispersions of SWNT–CTAB–Water at $9 \leq C_{CTAB} < 15$ wt % were imaged following different on-the-grid relaxation periods (0, 40, and 90 s). As was described earlier, micrographs of sheared samples prepared from dispersions of SWNT–CTAB–Water in this concentration range are dominated by long cylindrical CTAB micelles. The elongated micelles are aligned parallel to the longer SWNT (Figure 3A, 4A, 5B, and 8A). Cryo-TEM micrographs of specimens that were allowed to go through post-shear relaxation periods of 30–90 s show a qualitatively different structure. In the latter case, the dominant features are spherical micelles and short cylindrical micelles (Figure 8B) similar to those observed in native CTAB solution of similar concentration (Figure 3C and 5A). No evidence for micelles ordering is detected.

3. Discussion

In this study, we examined the phase behavior and nanostructure of the combined SWNT–CTAB–water system

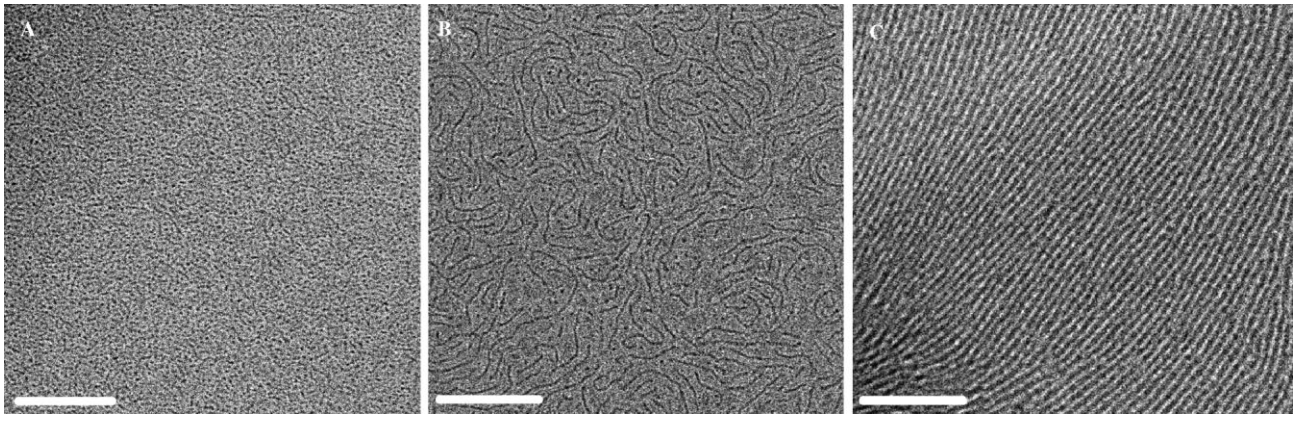

Figure 6. Cryo-TEM micrographs of CTAB solutions: A) 9 wt %, B) 12 wt %, C) 15 wt %. Scale bar 200 nm.

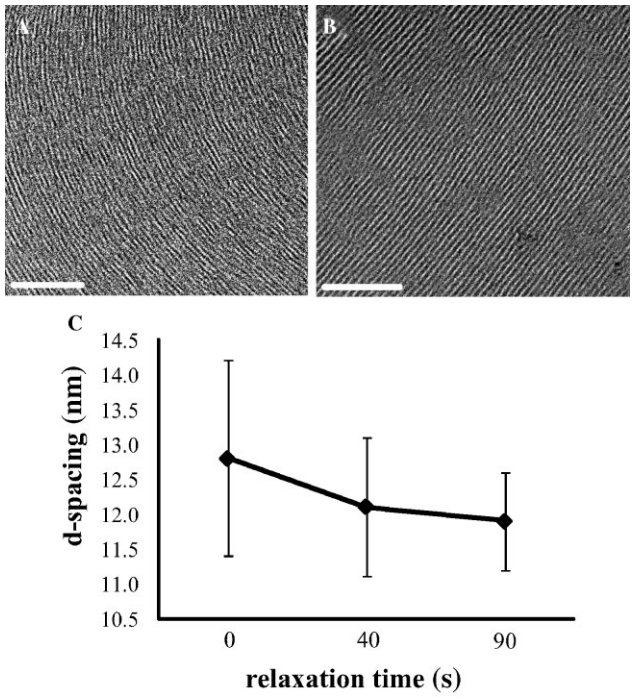

Figure 7. Cryo-TEM micrographs of C_{CTAB} (15 wt %)–water solution following post-blotting relaxation periods of A) 0 s, B) 90 s, and C) d-spacing and standard deviation following 0, 40, 90 s relaxation periods. Scale bar 200 nm.

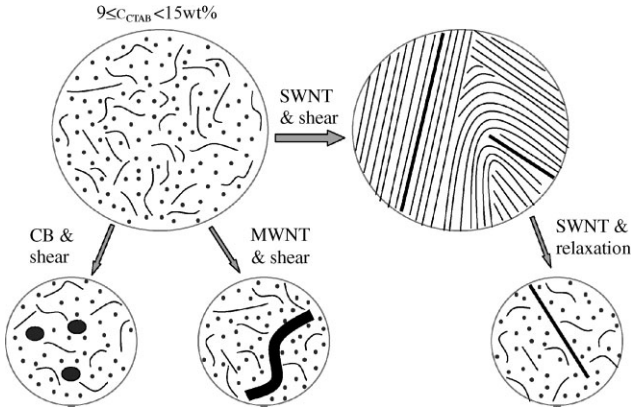

Figure 9. Schematic illustration of cryo-TEM micrographs of CTAB solutions at concentrations in the range of 9–12 wt %. The native solution contains a mixture of spherical and short cylindrical micelles. In the presence of low SWNT concentrations of (<1 wt %) SIS is observed. The elongated micelles are aligned with respect to the SWNT. On-the-grid relaxation results retain the native CTAB solution appearance. The presence of MWNT or CB does not result in a similar behavior. (Note that the schematic figure is not to scale.)

in bulk and thin films. Three significant effects were observed: 1) dispersed SWNT, MWNT, and CB were found to induce macroscopic phase separation and demixing in aqueous dispersions of CTAB while fullerenes did not. 2) Minute amounts of SWNT triggered SIS and elongated micelles ordering in nanometrically thin films of CTAB dispersions as schematically summarized in Figure 9. 3) SWNTs were incorporated into the fully ordered hexagonal lyotropic LC phase of CTAB while preserving the d-spacing of the native phase. In the following, we discuss the different effects in details.

3.1. Macroscopic Phase Behavior of Dispersions and Demixing

Our findings suggest that SWNT may be dispersed in aqueous solutions of CTAB over a wide concentration range, way above the CMC. This behavior is very different from the behavior of the commonly used anionic surfactant, sodium-dodecyl sulfate (SDS) where an upper surfactant limit for SWNT dispersion was observed, followed by coagulation of the tubes at high surfactant concentrations.[3] The CTAB dispersions were found to exhibit a rich phase behavior: for a given concentration of different carbonaceous additives (SWNT, MWNT, CB) a single phase was observed at low CTAB concentrations, a two-phase region was found at CTAB concentrations below the bulk LC phase of the surfactant, and a re-entrant single phase was observed at higher CTAB concentrations. The spontaneous demixing into two macroscopic liquid phases resulted in the formation of an upper transparent phase depleted of the nanotubes and a lower black phase enriched by SWNT (as indicated by SAXS (Figure 1C)). Cryo-TEM micrographs (Figure 3A, 4A, 5B, and 8) indicate that the SWNT residing in the lower phase are well dispersed. As mentioned earlier, the observed demixing is not unique to dispersions of SWNT, and characterizes dispersions of MWNT and CB at similar concentrations, but not of fullerenes.

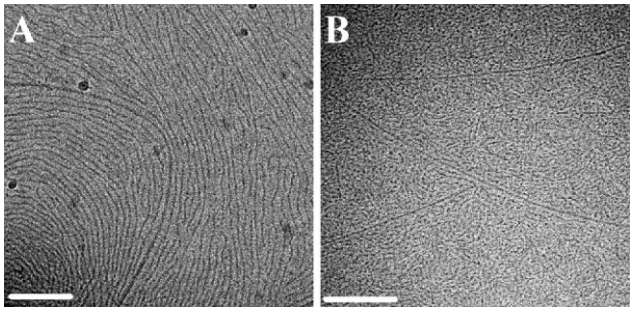

Figure 8. Cryo-TEM micrographs of C_{SWNT} (0.1 wt %)–C_{CTAB} (10 wt %)–water dispersion following relaxation periods of A) 0 s and B) 60 s. Scale bar 200 nm.

Recently, Poulin and coworkers[31] reported the observation of macroscopic phase separation in hyaluronic acid–SWNT–water system, and attributed the effect to excluded volume interactions. While in their case one of the phases was nematic, here both phases are bulk disordered phases. We suggest that the physical origin of the observed phase behavior is similar, and is related to entropic interactions leading to osmotic depletion forces.[32] Several studies of depletion-induced phase separation have been reported in colloidal systems.[33,34] Excluded volume interactions that drive the segregation of the additives are known to scale as the ratio of the typical length of the additive, L, to the micelle diameter, d, as d/L.[35] In our case, the typical diameter of the CTAB micelles (d) is ~5 nm. The length of a SWNT or a MWNT is of the order of a micron (or more), the diameter of CB particle is of the order of some tens of nanometers, and the diameter of a

small NANO MICRO

bare fullerene is of about 0.7 nm.[2,36] Consequentially, in all cases but that of the fullerenes, small values of d/L favor demixing, while the actual concentration at which demixing takes place would depend on the value of d/L. In addition, as the gain in free energy upon removing a particle of length L from the solution is of the order of the osmotic pressure times the gain in free volume, it would scale with L^3[35] and we would expect almost complete depletion of the additives from one of the phases, as indeed is observed (see inset in Figure 1). At higher CTAB concentrations, with the transition to the LC regime we observe a re-entrant single phase. This observation as well is consistent with the concentration dependence of a depletion potential between objects embedded within a solution of small spheres.

3.2. SIS and Orientational Ordering

Nanometrically thin films prepared from the lower phase of the SWNT–CTAB–water dispersions by applying a strong shear action were inspected using cryo-TEM. In the presence of SWNT, long-range ordering of elongated micelles was clearly observed at $C_{CTAB} > 9$ wt %. The effect was found to be exclusive to SWNT, and similar SIS was not observed in the presence of MWNT and CB.

The major finding presented here is that under the action of shear, SWNT nucleate the formation of a well-aligned phase of elongated CTAB micelles, at low concentrations. The ordered regions extend over microns. The effect is unique to SWNT, and investigation of other carbonaceous additives of similar composition and surface area (MWNT, CB) but different diameter (MWNT) or geometry (CB) did not reveal a similar behavior. For $C_{SWNT} = 0.1$ wt %, SIS was observed at a CTAB concentrations of $9 \leq C_{CTAB} < 15$ wt %. Native CTAB solutions at these concentrations were not found to align in response to shear.

At higher CTAB concentrations ($C_{CTAB} = 15$ wt %) a native ordered phase composed of well-aligned elongated micelles was observed (Figure 7). Here, in the native system without additives, the major effect of exposure to shear is compaction of the packing of the micelles (smaller d-spacing).

Probably the most striking observation is the difference in the response of the system to the presence of SWNT as compared to MWNT. While both are elongated cylindrical structures of similar composition, surface energy, and aspect ratio, CTAB-coated SWNT mimic closely an elongated CTAB micelle, presenting a diameter of 5 nm (see Table S1 Supporting Information) and exposing to the surrounding a structure of a closely packed CTAB micelle, yet, with a higher persistence length. We suggest that the major effect of SWNT is to serve as a nucleating agent. Their main action, we believe, is to facilitate the transition to the highly aligned phase of CTAB micelles, similar to that observed in the native solution at a higher CTAB concentration (see Figure 7). A similar effect is not observed in the presence of MWNT where the relatively large diameter of the tube (>20 nm) excludes the possibility of mimicking an elongated CTAB micelle (5 nm in diameter). Thus, it is the unique combination of geometric and dimensional similarity to the CTAB micelles, and the rigidity of the CTAB-coated SWNTs that lead to shear-induced ordering and alignment of micelles over mesoscopically large areas.

Indeed, we suggest that upon shear SWNTs nucleate elongated well-aligned micelles along a vector set by the embedded SWNTs (Figures 3A, 5B, and 8A). Relaxation leads to disappearance of the aligned phase (Figure 8B) and the sample assumes an unordered state. At similar concentrations, thin films of the native solutions (without SWNT) do not order upon shearing, and it is only above $C_{CTAB} = 15$ wt % that ordering commences (Figure 7). These findings bear great potential for the design of ordered arrays of functional materials such as chromophores, where dispersed SWNT may induce orientational ordering in thin films. The necessary requirements (i.e., chemical composition, chemical structure, etc.) depend on the specific parameters of the additive in question and should be tailored accordingly.

3.3. SWNT and Ordered Lyotropic LC Phase of CTAB

SAXS measurements (Figure 2) of CTAB solutions at concentrations >22 wt % clearly indicate that SWNT are incorporated into the fully ordered lyotropic LC phase without affecting the spacing of the native phase, while CB does not. Here again, good matching between the surfactant-coated SWNT and the native structures is believed to be the origin of the observed behavior.

4. Conclusions

We found that carbonaceous additives of mesoscopic and nanometric dimensions induce demixing and macroscopic phase separation in otherwise homogeneous solutions of CTAB, via entropic excluded volume interactions. Minute concentrations of SWNT were found to nucleate the appearance of an oriented surfactant phase in nanometrically thin films prepared from dispersions of individual SWNT, under the action of external shear. The effect was found to be exclusive to SWNT, and occurred at SWNT concentrations well below those relevant to tube-tube ordering. SWNT are found to incorporate into the ordered LC (equilibrium) phases of the native surfactant at high surfactant concentrations.

The assembly and ordering of the combined surfactant-SWNT may offer a simple pathway for engineering the structure of nanometrically thin films on different substrates.

5. Experimental Section

Materials: Raw SWNT synthesized by arc discharge were purchased from Carbolex, Inc. USA (http://carbolex.com) (SWNT (AP) batch no: CLAP8420) and used as received. MWNT produced by Catalytic Chemical Vapor Deposition were purchased from INP (Toulouse, France). A dry powder of CB, Vulcan P grade, was purchased from Cabot Corp., USA, and used as received. Fullerene (Buckminsterfullerene product no. 37 964–6 99.5% purity) was purchased from Sigma–Aldrich, Israel. CTAB (product no. H5882-

100G, 99% purity) was purchased from Sigma (Israel) and used as received.

Sample preparation: Aqueous solutions of CTAB in concentrations of 0.5–30 wt % (CTAB in water) were prepared by dissolving the surfactant in water (Millipore water, resistance of 18.2 MΩ cm) at room temperature (25 °C). The solutions were incubated for at least 2 days before being used.

Liquid dispersions of SWNT, MWNT, and CB were prepared by sonicating the powder of the raw material (typical concentration of 0.1–1.0 wt %) at very mild conditions[37,38] (mini supersonic cleaner, Delta DG-1, 50 W, 43 kHz) for 30–40 min in 1 wt % CTAB solution. The dispersions were centrifuged (at 4500 rpm for 30 min) and the supernatant was decanted from above the precipitate. Dispersions in higher CTAB concentrations were prepared by adding CTAB to the dispersion.

Techniques: SAXS measurements were performed using a Ni-filtered Cu KR radiation of 0.15418 nm operated at 40 kV, 40 mA (Seifert ID 3000 generator). A linear position-sensitive detector (MBraun) was used to record the scattering patterns. The scattering vector, q, is defined independent of radiation wavelength:

$$q = \frac{4\pi}{\lambda}\sin\frac{\theta}{2} \quad (1)$$

Samples were prepared by filling thin glass capillaries (1.5 mm in diameter) and sealing them with epoxy.

TEM at cryogenic temperature (Cryo-TEM) was used for direct imaging of the solutions and dispersions.[23,39,40]

The specimens studied via cryo-TEM are prepared as described previously.[23] Solution (or dispersion) drops of typically 5 μL are deposited on perforated polymer film supported on a 300 mesh carbon coated EM grid (copper, Ted Pella – lacey substrate). Ultra-thin films (10–250 nm) are formed by removing most of the solution by blotting. The process is carried out in a controlled environment vitrification system where the temperature and the relative humidity are controlled, using an automatic system termed Vitrobot (FEI). The samples were examined at −178 °C using an FEI Tecnai 12 G^2 TWIN TEM equipped with a Gatan 626 cold stage (at the Ilse Katz Institute for Nanoscale Science and Technology Ben-Gurion University of the Negev, Beer Sheva, Israel).

Acknowledgements

E. N.-R. would like to acknowledge the support of the Women in Science scholarship of the Israel Ministry of Science and Technology. R. Y.-R. acknowledges that support of the Israel Science Foundation (grant no. 512/06).

[1] P. M. Ajayan, T. W. Ebbesen, *Rep. Prog. Phys.* **1997**, *60*, 1025.
[2] M. S. Dresselhaus, S. G. Dresselhau, P. C. Eklund, *Science of Fullerenes and Carbon Nanotubes: Their Properties and Applications*, Academic Press, Orlando, FL 1996.
[3] B. Vigolo, A. Penicaud, C. Coulon, C. Sauder, R. Pailler, C. Journet, P. Bernier, P. Poulin, *Science* **2000**, *290*, 1331.
[4] O. Regev, P. N. B. ElKati, J. Loos, C. E. Koning, *Adv. Mater.* **2004**, *16*, 248.
[5] L. Vaisman, H. D. Wagner, G. Marom, *Adv. Colloid Interface Sci.* **2006**, *128*, 37.
[6] V. K. Gupta, J. J. Skaife, T. B. Dubrovsky, N. L. Abbott, *Science* **1998**, *279*, 2077.
[7] R. R. Shah, N. L. Abbott, *Science* **2001**, *293*, 1296.
[8] J. M. Brake, M. K. Daschner, Y. Y. Luk, N. L. Abbott, *Science* **2003**, *302*, 2094.
[9] V. Weiss, R. Thiruvengadathan, O. Regev, *Langmuir* **2006**, *22*, 854.
[10] L. Ramos, P. Fabre, E. Dubois, *J. Phys. Chem.* **1996**, *100*, 4533.
[11] O. Regev, R. Backov, C. Faure, *Chem. Mater.* **2004**, *16*, 5280.
[12] L. Ramos, P. Fabre, R. Ober, *Eur. Phys. J. B* **1998**, *1*, 319.
[13] W. Wang, S. Efrima, O. Regev, *J. Phys. Chem. B* **1999**, *103*, 5613.
[14] C. Quilliet, V. Ponsinet, V. Cabuil, *J. Phys. Chem.* **1994**, *98*, 3566.
[15] *Small-Angle Scattering and Light Scattering in Neutron, X-ray, and Light Scattering* (Eds.: O. Glatter, Th. Zemb, P. Linder), North Holland, **1991**.
[16] B. D. Cullity, *Elements of X-ray Diffraction*, Addison-Wesley, Upper Saddle River, NJ **1978**.
[17] X. Auvray, C. Petipas, R. Anthore, I. Rico, A. Lattes, *J. Phys. Chem.* **1989**, *93*, 7458.
[18] T. Warnheim, A. Jonsson, *J. Colloid Interface Sci.* **1988**, *125*, 627.
[19] E. Cappelaere, R. Cressely, J. P. Decruppe, *Colloid Surf. A* **1995**, *104*, 353.
[20] E. Cappelaere, R. Cressely, *J. Phys. II* **1995**, *5*, 1611.
[21] Characteristic SAXS curves of CTAB solutions in concentrations 9–21 wt % are presented in Figure S1 in the Supporting Information.
[22] D. Danino, Y. Talmon, R. Zana, *Coll. Surf. A* **2000**, *169*, 67.
[23] Y. Talmon, *Ber. Bunsen-Ges. Phys. Chem. Chem. Phys.* **1996**, *100*, 364.
[24] Y. Zheng, Z. Lin, J. L. Zakin, Y. Talmon, H. T. Davis, L. E. Scriven, *J. Phys. Chem. B* **2000**, *104*, 5263.
[25] a) F. Braet, E. Wisse, P. Bomans, P. Frederik, W. Geerts, A. Koster, L. Soon, S. Ringer, *Microsc. Res. Tech.* **2007**, *70*, 230; b) http://www.fei.com/Products/Types/SpecialtyTools/tabid/240/Default.aspx (accessed June 2008).
[26] C. V. Iancu, W. F. Tivol, J. B. Schooler, D. P. Dias, G. P. Henderson, G. E. Murphy, E. R. Wright, Z. Li, Z. H. Yu, A. Briegel, L. Gan, Y. N. He, G. J. Jensen, *Nat. Protoc.* **2006**, *1*, 2813.
[27] O. Regev, F. Guillemet, *Langmuir* **1999**, *15*, 4357.
[28] C. Taschner, F. Pacal, A. Leonhardt, P. Spatenka, K. Bartsch, A. Graff, R. Kaltofen, *Surf. Coat. Technol.* **2003**, *174*, 81.
[29] Films formed by blotting CTAB solutions of concentrations above CCTAB = 15 wt % are too thick to be imaged by cryo-TEM since the solutions are very viscous and the electron beam cannot penetrate the film. [*Cryotechniques in Biological Electron Microscopy. Electron Beam Radiation Damage to Organic and Biological Cryo-Specimens*, Springer Verlag, Heidelberg, Germany **1987**].
[30] The d-spacings were calculated by averaging the spacing of repeating distances over tens of micrographs.
[31] S. E. Moulton, M. Maugey, P. Poulin, G. G. Wallace, *J. Am. Chem. Soc.* **2007**, *129*, 9452.
[32] Assuming that the overall concentration of CTAB molecules is quite similar in the upper and lower phase, and that about 5% of the CTAB molecules are adsorbed onto the carbonaceous species (in accordance with previous studies (C. Richard, F. Balavoine, P. Schultz, T.W. Ebbesen, C. Mioskowski *Science* **2003**, *300*, 775) the effective concentration of the free CTAB micelles in the lower phase may be lower by about 0.5 wt % as compared to the upper phase.
[33] W. C. K. Poon, P. B. Warren, *Europhys. Lett.* **1994**, *28*, 513.

[34] H. Gang, A. H. Krall, D. A. Weitz, *Phys. Rev. Lett.* **1994**, *73*, 3435.
[35] R. A. L. Jones, *Soft Condensed Matter*, 1st edition, Oxford University Press, Oxford **2002**.
[36] We assume that a fullerene coated by CTAB have an effective diameter of about 3–4 nm.
[37] R. Shvartzman-Cohen, E. Nativ-Roth, E. Baskaran, Y. Levi-Kalisman, I. Szleifer, R. Yerushalmi-Rozen, *J. Am. Chem. Soc.* **2004**, *126*, 14850.
[38] R. Shvartzman-Cohen, Y. Levi-Kalisman, E. Nativ-Roth, R. Yerushalmi-Rozen, *Langmuir* **2004**, *20*, 6085.
[39] D. Danino, A. Bernheim-Groswasser, Y. Talmon, *Colloid Surf. A* **2001**, *183*, 113.
[40] E. Buhler, C. Oelschlaeger, G. Waton, M. Rawiso, J. Schmidt, Y. Talmon, S. J. Candau, *Langmuir* **2006**, *22*, 2534.

Received: January 17, 2008

